Meteoritics & Planetary Science 40, Nr 11, 1635–1652 (2005)
Abstract available online at http://meteoritics.org

Spallation recoil II: Xenon evidence for young SiC grains

U. OTT[1*], M. ALTMAIER[1†], U. HERPERS[2], J. KUHNHENN[2‡],
S. MERCHEL[1††], R. MICHEL[3], and R. K. MOHAPATRA[1‡‡]

[1]Max-Planck-Institut für Chemie, Becherweg 27, D-55128 Mainz, Germany
[2]Universität zu Köln, D-50674 Köln, Germany
[3]Universität Hannover, D-30167 Hannover, Germany
[†]Present address: Forschungszentrum Karlsruhe, D-76021 Karlsruhe, Germany
[‡]Present address: Fraunhofer IT, D-53879 Euskirchen, Germany
[††]Present address: Bundesanstalt für Materialforschung und -prüfung, D-12205 Berlin, Germany
[‡‡]Present address: Department of Earth Sciences, University of Manchester, M13 9PL, Manchester, UK
[*]Corresponding author. E-mail: ott@mpch-mainz.mpg.de

(Received 27 September 2004; revision accepted 09 August 2005)

Abstract–We have determined the recoil range of spallation xenon produced by irradiation of Ba glass targets with ~1190 and ~268 MeV protons, using a catcher technique, where spallation products are measured in target and catcher foils. The inferred range for ^{126}Xe produced in silicon carbide is ~0.19 μm, which implies retention of ~70% for ^{126}Xe produced in "typical" presolar silicon carbide grains of 1 μm size. Recoil loss of spallation xenon poses a significantly smaller problem than loss of the spallation neon from SiC grains. Ranges differ for the various Xe isotopes and scale approximately linearly as function of the mass difference between the target element, Ba, and the product. As a consequence, SiC grains of various sizes will have differences in spallation Xe composition. In an additional experiment at ~66 MeV, where the recoil ranges of ^{22}Na and ^{127}Xe produced on Ba glass were determined using γ-spectrometry, we found no evidence for recoil ranges being systematically different at this lower energy. We have used the new data to put constraints on the possible presolar age of the SiC grains analyzed for Xe by Lewis et al. (1994). Uncertainties in the composition of the approximately normal Xe component in SiC (Xe-N) constitute the most serious problem in determining an age, surpassing remaining uncertainties in Xe retention and production rate. A possible interpretation is that spallation contributions are negligible and that trapped ^{124}Xe/^{126}Xe is ~5% lower in Xe-N than in Q-Xe. But also for other reasonable assumptions for the ^{124}Xe/^{126}Xe ratio in Xe-N (e.g., as in Q-Xe), inferred exposure ages are considerably shorter than theoretically expected lifetimes for interstellar grains. A short presolar age is in line with observations by others (appearance, grain size distribution) that indicate little processing in the interstellar medium (ISM) of surviving (crystalline) SiC. This may be due to amorphization of SiC in the ISM on a much shorter time scale than destruction, with amorphous SiC not surviving processing in the early solar system. A large supply of relatively young grains may be connected to the proposed starburst origin (Clayton 2003) for the parent stars of the mainstream SiC grains.

INTRODUCTION

Presolar grains found in primitive meteorites constitute a link between astrophysics, cosmochemistry, and meteorite research (e.g., Bernatowicz and Zinner 1997; Ott 2003). Grains identified up to now mostly comprise extremely refractory and chemically resistant mineral types (e.g., Hoppe and Zinner 2000), including graphite, diamond, silicon carbide, silicon nitride, and refractory oxides. Although abundant in the interstellar medium (e.g., Draine 2003; Whittet 2003), presolar silicates have only recently been proven to be present in interplanetary dust particles (Messenger et al. 2003) and in meteorites (Nguyen and Zinner 2004; Nagashima et al. 2004; Mostefaoui and Hoppe 2004).

One of the major unresolved questions concerning presolar grains in meteorites is their age. Reliable information on this topic may provide crucial information concerning several astrophysical questions. Typical lifetimes of

refractory interstellar grains are of fundamental importance. They are directly relevant when considering the efficiency of grain destruction and the balance between input of new dust and its destruction (Jones et al. 1994, 1997; see below). Also, ages for presolar grains with signature isotopic abundances that imply specific stellar sources may place meaningful constraints on models of galactic chemical evolution.

Astrophysical considerations have led to the conclusion that the destruction of dust grains in the interstellar medium is mostly due to supernova shock waves in the warm neutral/ionized medium (Jones et al. 1994, 1997). Lifetimes have been estimated at ~600 Ma and ~400 Ma for graphite and silicate grains, respectively (Jones et al. 1997), and although estimates range as high as ~1.5 Ga for silicon carbide grains (Bernatowicz et al. 2003), these ages are significantly shorter than the typical stardust injection time scale (Jones et al. 1997). For this reason and in order to account for the observed depletion in the gas phase of refractory elements, the existence of an effective grain growth mechanism in the interstellar medium has been postulated. Given that no such process has been identified so far (e.g., Whittet 2003), independent information about typical lifetimes of interstellar grains is essential for testing grain growth mechanisms. A reliable age for the presolar grains in primitive meteorites may also bear on the hypothesis that some fraction of the grains originated in a recent event (supernova, AGB stars) that triggered formation of the solar system (Foster and Boss 1996; Boss and Foster 1997).

Determining an age for interstellar grains is not straightforward, however. Conventional radiometric dating is difficult. Given the large isotope abundance anomalies observed in presolar grains, we can neither be certain about the initial abundance of the parent nor the daughter nuclide. An alternative technique is to determine the time the grains have been exposed to the cosmic radiation in the interstellar medium (Tang and Anders 1988a, 1988b). The approach can be most usefully applied to silicon carbide grains. First attempts have concentrated on spallation Ne, which is abundantly produced from silicon. We have demonstrated, however, that the ages of Tang and Anders (1988b) and Lewis et al. (1990, 1994) are compromised, because the extent of recoil loss of spallation Ne from the typically μm-sized SiC grains is significantly larger than assumed (Ott and Begemann 2000). Only the very largest grains would quantitatively retain spallation neon. At the same time we suggested that analysis of spallation xenon (produced mostly on the relatively abundant Ba in the SiC grains) instead of neon might be largely free from this source of uncertainty.

Here we report on the recoil range of spallation xenon produced by proton irradiation of Ba glass targets and the implications of these measurements for presolar SiC grains. In our previous work on recoil of spallation Ne (Ott and Begemann 2000), we measured the Ne retained in SiC grains in the ~1 to ~5 μm size range. The results were consistent with predictions based on literature data for similar systems, e.g., ^{24}Na and ^{22}Na produced on Al targets (Steinberg and Winsberg 1974). For these nuclides, the "catcher technique" had been employed. Accordingly, we have used this (simpler) technique for our Xe measurements. Catcher foils containing spallation recoil products were available from two previous experiments in which a variety of targets (in the stacked-foil technique) had been irradiated by protons (initial energy 330 and 1200 MeV, respectively). Xe had been measured in one of the Ba targets in earlier work (Mathew et al. 1994); the other was available for this work. We also performed an additional irradiation at ~71 MeV (initial energy). Preliminary results have been presented in abstracts (Mohapatra et al. 2001; Ott et al. 2001).

PROCEDURES

Irradiation and Samples

Spallation xenon from Ba was produced by irradiating Ba glass (composition: 40.2% Ba, 35.9% O, 16.3% Si, 4.5% B, and 3.0% Al by weight) with protons. The thickness of the glass targets was ~3.25 mm, the density ~3.4 g/cm^3, for a typical weight of ~2 g. Irradiations with protons of 1200 and 330 MeV energy were performed at the Laboratoire National Saturne, Saclay (France). This specific work is part of a larger experimental setup, in which the stacked-foil technique was used to study the production of cosmogenic nuclides (Michel et al. 1995; Schiekel et al. 1996; Gloris et al. 2001). Irradiation with 71 MeV protons was performed at Paul Scherrer Institute, Villigen (Switzerland), using similar methods. The proton energies at the position of the Ba targets inside the stacks were ~1190, ~268, and ~66 MeV; we nevertheless refer to the three irradiations as 1200, 330, and 71 MeV irradiation in the following. The corresponding fluences were 2.31×10^{15}, 1.64×10^{14}, and 1.34×10^{16} protons cm^{-2}, respectively.

The Ba glass targets in the high energy irradiations (a pair in the case of the 1200 MeV irradiation) were sandwiched between Al catcher foils which collected the recoil nuclei from the Ba glass targets. Two identical targets were mounted behind each other in the 1200 MeV irradiation. The Xe in one of these was analyzed by Mathew et al. (1994). Their results are used, together with the results of our own Al catcher foil measurements, in the calculation of recoil ranges. We measured recoil nuclei emitted in the backward position from this target and those emitted in the forward position by its twin. In the 71 MeV irradiation, we used graphite as a catcher material instead of Al because we also wanted to study the recoil of ^{22}Na produced at this low energy in order to compare with the previously determined ^{21}Ne recoil at 1.6 GeV proton energy (Ott and Begemann 2000). A summary of the measurements and materials studied in this work is given in Table 1.

Table 1. Samples investigated for spallation recoil range.

Sample name	Proton beam energy (MeV)[a]	Material, thickness	Analyzed products	Comments
CS1141	1200 (1190)	Al, 125 μm	Stable Xe isotopes	Backward recoils
CS1151	1200 (1190)	Al, 125 μm	Stable Xe isotopes	Forward recoils
ALSH183	330 (268)	Al, 125 μm	Stable Xe isotopes	Backward recoils
BGSH181	330 (268)	Ba glass[b], 3.2 mm	Stable Xe isotopes	Ba target
ALSH184	330 (268)	Al, 500 μm	Stable Xe isotopes	Forward recoils
CCZM012	71 (66)	Graphite, 125 μm	^{22}Na, ^{127}Xe	Backward recoils
BGZM011	71 (66)	Ba glass[b], 3.2 mm	^{22}Na, ^{127}Xe	Si, Ba target
CCZM021	71 (66)	Graphite, 125 μm	^{22}Na, ^{127}Xe	Forward recoils
CCZM022	71 (66)	Graphite, 125 μm	^{22}Na, ^{127}Xe	Blank

[a]Both initial beam energy and, in parentheses, energy at the target are given.
[b]Major elements (wt%) of Ba glass: 40.2% Ba, 35.8% O, 16.2% Si, 4.5% B, 3.0% Al, and 0.3% Sr.

Measurement of Spallation Products

Stable Xe Measurements

Xenon produced in the Ba glass from the 330 MeV irradiation as well as Xe in the Al catcher foils of both the 1200 and 330 MeV experiments was measured by standard procedures in our laboratory (e.g., Schelhaas et al. 1990; Ott and Begemann 2000).

Barium Glass

To avoid excessive memory from large amounts of spallation xenon in the mass spectrometer, the 330 MeV Ba target (total weight 1.86 g) was not measured in toto. Instead the glass was finely crushed and only three small fractions (<1.2 mg) were analyzed. Since spallation Xe concentrations found for each of the three glass powder splits were within <10% of the mean (see results below), we conclude that they are representative for the entire Ba glass. For the remainder of the discussion we use the weighted average.

Gas Extraction

Catcher foil ALHS183 (Table 1) as well as the glass samples were wrapped in Ni foil and heated in a W crucible inside a Ta tube, while the three other catchers were wrapped in Pt foil and heated inside an Ir tube. Extraction from the Al foils did not require high temperature. In the first of the foil runs (CS1151) ~90% of spallation gas was found to be released at 700 °C nominal oven temperature, with the remaining 10% at 800 °C. Subsequent foil extractions were at 800° C only. Similarly, since the first split of Ba glass was found to be totally degassed by heating at 1400 °C (no spallation Xe released in subsequent 1500 °C heating), the two remaining splits were degassed at 1400 °C. For all analyses pre-heating steps to remove adsorbed gases were employed (250 °C for the catcher foils, 500 °C for the glass target splits), with no measurable release of spallation products.

Calculation of Spallation Component

To obtain the spallation Xe component in the glass and the catchers we subtracted from the mass discrimination corrected data an "effective blank," comprising both extraction blank and Xe indigenous to and/or still adsorbed to the materials after the pre-heating steps. Since our Xe extraction blanks were isotopically indistinguishable from atmospheric Xe, this was done by assuming all of ^{136}Xe to be of "blank" origin and assuming the "blank" to have terrestrial atmospheric composition. For the "typical" spallogenic isotopes ^{124}Xe and ^{126}Xe, the correction generally was negligible. For ^{128}Xe and ^{130}Xe, the other two isotopes of interest within our later discussion, corrections amounted to ~6 and ~19% for the 1200 MeV irradiation, while for the 330 MeV irradiation they were too large to calculate meaningful abundances of backward recoils.

γ-ray Spectrometry

Because of the low Xe nuclide production in the 71 MeV irradiation, we measured the activity of radioactive ^{127}Xe ($T_{½}$ = 36 d). This was done by standard γ-ray spectrometry at University of Cologne (e.g., Bodemann et al. 1993; Schiekel et al. 1996; Gloris et al. 2001; and references therein). The ^{127}Xe activities were also rather low and of limited value. Together with ^{127}Xe, we also measured the ^{22}Na activity of the sample and catcher foils (graphite in this case), together with a "blank" graphite foil exposed to the beam but shielded from recoil nuclei.

RESULTS

Cross-Sections

In addition to serving as the base line for determining recoil losses, data obtained for the targets of the 71 and 330 MeV irradiations also add to the existing database of cross-section measurements.

71 MeV Irradiation

Measured count rates for the Ba glass target as well as the catchers are listed in Table 2. Calibrated with the efficiency of our HPGe detector, the ^{127}Xe count rate corresponds to an

Table 2. Activities of ^{22}Na and ^{127}Xe in Ba glass target and catcher foils for 71 MeV irradiation as counted 110 days after end of irradiation. Uncertainties (in percent) given in parentheses are based on counting statistics only.

Sample name	Sample	^{22}Na (cps)	^{127}Xe (cps)
CCZM012	Backward graphite catcher	0.003 (20%)	<0.005
BGZM011	Ba glass target	29 (1%)	12.2 (1%)
CCZM021	Forward graphite catcher	0.016 (11%)	<0.005
CCZM022	Graphite blank	0.0025 (21%)	<0.005

activity of (22.0 ± 1.3) kBq at the end of irradiation. Given a sample mass of 2.05 g, a Ba content of 40.2% (by weight) and a proton fluence of 1.34 × 10^{16} cm^{-2}, the inferred cross-section for production of ^{127}Xe by 65.8 MeV protons from Ba is (2.07 ± 0.19) mb. The error reflects uncertainties in weight, composition and, most importantly, fluence. This result is consistent with existing data, being about 11% lower than the corresponding value obtained from an interpolation between the 64.6 and 66.5 MeV cross-sections in the Michel et al. (1997) database. Given the steepness of the excitation function in this energy region and the uncertainties in the actual energy in the two sets of experiments this slight difference is not surprising.

330 MeV Irradiation

Using the weighted mean of the concentration measurements from the three splits (Table 3) and a fluence of 1.64 × 10^{14} p cm^{-2} results in a cross-section for ^{126}Xe production from Ba by protons of energy 268 MeV of (59.9 ± 7.4) mb. The uncertainties include the analytical uncertainty of the Xe measurement, the uncertainty of the fluence and an assumed 5% uncertainty in the amount of calibration gas. The result is compared with other measurements in the 100 to 2600 MeV range in Fig. 1. It is higher than the value obtained by Kaiser (1977) at 300 MeV, and even higher than the Mathew et al. (1994) value for 600 MeV obtained at PRL. It is lower, however, than the cross-section inferred from the 600 MeV target measurement at MPI (Mathew et al. 1994). Still, the differences are modest, and our new value compares favorably with the trend of the most recently obtained data set, that of Gilabert et al. (1997). Most importantly, the comparison shows that our method of measuring spallogenic gases on only small splits of the target leads to reliable data.

For isotopic ratios of spallation Xe the situation is similar. A comparison is made in Fig. 2. On the left we compare our Xe isotope ratios (plotted at the true energy at the Ba target of 268 MeV) to those obtained by Kaiser (1977) in the energy range ~100 to 600 MeV (data points connected by a line); on the right, our values are the left-most points and are compared to the higher-energy PRL data of Mathew et al. (1994). The data are in agreement, given the uncertainties in the true proton energies at the target; except for ^{134}Xe, almost

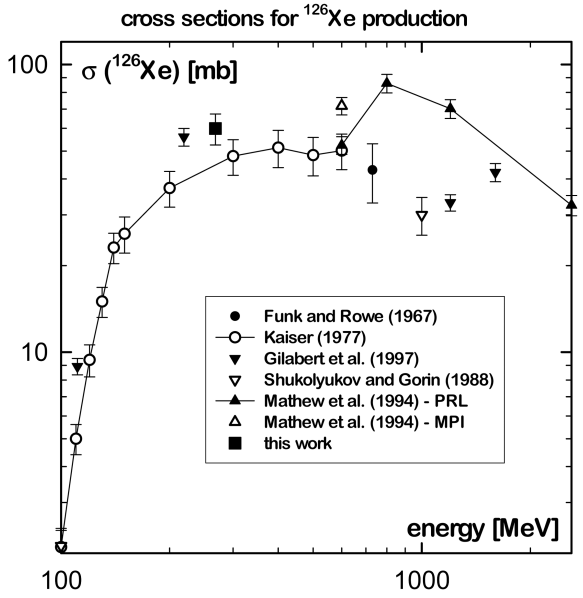

Fig. 1. Comparison of cross-sections for ^{126}Xe spallation production by proton irradiation of Ba. The value obtained in this work (330 MeV irradiation, 268 MeV at the target) is compared with literature values (Funk and Rowe 1967; Kaiser 1977; Shukolyukov and Gorin 1988; Mathew et al. 1994; Gilabert et al. 1997).

perfect agreement with the Kaiser data is achieved if we assume the true energy in their 300 MeV experiment to have been about 10% lower.

Recoil Ranges

Calculation of Recoil Ranges

The relevant data for calculating an effective recoil range are the relative amounts of spallation atoms in the forward and backward catcher foils and the thickness of the target. In calculating the ranges reported in our preliminary reports (Mohapatra et al. 2001; Ott et al. 2001), we have used equations given by Sugarman et al. (1956):

$$R = 4W \times F/(1+\eta)^2 \quad (1)$$

or alternatively:

$$R = 4W \times B/(1+\eta)^2 \quad (2)$$

where R = recoil range, W = thickness of the target, F and B = fraction of recoils in the forward and backward direction, respectively, and

$$\eta = [(F/B)^{1/2} - 1]/[(F/B)^{1/2} + 1] \quad (3)$$

The classical model for the interaction of high-energy protons with medium to heavy nuclei is a two step model (e.g., Lagarde-Simonoff et al. 1976). The first step is that of ejection of prompt nucleons and formation of an intermediate excited residual nucleus. This is followed by de-excitation of/

Table 3. Xe abundances and isotopic compositions measured in Ba glass target BGSH 181 irradiated with 330 MeV protons.

Split #, weight	$^{132}Xe_m$ (10^{-15} cc)	$^{126}Xe_s$ (10^{-10} cc/g)	^{124}Xe	^{126}Xe	^{128}Xe	^{129}Xe	^{130}Xe	^{131}Xe	^{132}Xe	^{134}Xe	^{136}Xe
1, 1.13 mg	412 (21)		1.081(22)	1.815(40)	2.305(37)	2.577(44)	1.181(21)	2.739(47)	≡1	0.078(4)	0.042(3)
Spallogenic		6.61 (39)	0.596(18)	≡1	1.265(35)	1.352(40)	0.641(18)	1.455(42)	0.482(14)	0.016(4)	≡0
2, 0.85 mg	274 (15)		1.081(26)	1.817(37)	2.372(54)	2.696(96)	1.215(21)	2.841(74)	≡1	0.082(7)	0.045(4)
Spallogenic		5.81 (35)	0.595(19)	≡1	1.301(40)	1.410(62)	0.657(18)	1.505(52)	0.476(14)	0.016(5)	≡0
3, 0.053 mg	36 (2)		0.517(23)	0.921(33)	1.240(68)	1.874(92)	0.746(48)	1.968(88)	≡1	0.302(36)	0.283(54)
Spallogenic		6.20 (63)	0.559(32)	≡1	1.284(90)	1.120(233)	0.671(67)	1.405(200)	0.153(205)	–0.035(88)	≡0
Sum	722 (26)		1.053(16)	1.771(27)	2.278(30)	2.587(45)	1.172(14)	2.740(39)	≡1	0.091(4)	0.055(4)
Spallogenic		6.28 (25)	0.595(13)	≡1	1.280(26)	1.369(34)	0.648(13)	1.473(33)	0.471(12)	0.015(4)	≡0

First line for each sample: as measured, corrected for mass discrimination only, normalized to $^{132}Xe \equiv 1$.
Second line: derived spallation Xe abundance and composition (see text for details); normalized to $^{126}Xe \equiv 1$.
"Sum" is the weighted mean of the three splits derived from the summed raw data. Uncertainties in the last digits are given in parentheses.

Table 4. Xe abundances and isotopic compositions measured in Al catcher foils.

Sample name	$^{132}Xe_m$ (10^{-15} cc)	$^{126}Xe_s$ (10^{-15} cc)	^{124}Xe	^{126}Xe	^{128}Xe	^{129}Xe	^{130}Xe	^{131}Xe	^{132}Xe	^{134}Xe	^{136}Xe
1200 MeV irradiation											
CS1141	96 (3)		0.650(33)	0.844(30)	0.907(46)	1.297(71)	0.590(87)	1.095(96)	≡1	0.307(20)	0.239(80)
spallogenic		81(4)	0.769(48)	≡1	1.016(70)	0.695(304)	0.571(115)	0.622(261)	0.328(295)	0.031(117)	≡0
CS1151 (1)	187 (4)		4.122(93)	4.555(91)	4.018(79)	3.980(72)	1.386(100)	3.270(64)	≡1	0.151(10)	0.090(10)
spallogenic		851 (32)	0.905(27)	≡1	0.878(25)	0.815(25)	0.295(23)	0.671(21)	0.160(9)	0.010(4)	≡0
CS1151 (2)	51 (2)		1.252(81)	1.321(53)	1.313(36)	1.742(101)	0.416(69)	1.535(120)	≡1	0.351(10)	0.189(60)
spallogenic		68 (3)	0.948(72)	≡1	0.964(49)	0.893(167)	0.249(58)	0.821(151)	0.323(145)	0.098(56)	≡0
CS1151 sum	238 (7)		3.502(78)	3.857(76)	3.434(66)	3.497(62)	1.176(80)	2.895(59)	≡1	0.194(8)	0.111(15)
spallogenic		919 (32)	0.908(27)	≡1	0.884(24)	0.821(27)	0.292(22)	0.682(24)	0.172(14)	0.016(6)	≡0
330 MeV irradiation											
ALSH183	232 (23)		0.010(3)	0.014(2)	0.082(9)	0.969(32)	0.157(18)	0.783(24)	≡1	0.384(15)	0.320(16)
spallogenic		2.4 (0.6)	0.60(27)	≡1	1.2(1.8)	–	–	–	–	–	≡0
ALSH184	121 (9)		0.489(17)	0.662(17)	0.639(26)	1.455(52)	0.344(34)	1.080(30)	≡1	0.346(12)	0.268(10)
spallogenic		80 (6)	0.738(33)	≡1	0.882(48)	0.993(174)	0.334(58)	0.663(131)	0.281(152)	0.046(62)	≡0

First line for each sample: as measured, corrected for mass discrimination only; normalized to $^{132}Xe \equiv 1$.
Second line: derived spallation Xe abundance and composition (see text for details); normalized to $^{126}Xe \equiv 1$.
Uncertainties in the last digits are given in parentheses. For CS1151 spallation Xe was released in two temperature steps, which are listed individually together with the sum. For the others spallation Xe was released in a single step (see experimental details). Because of the low amounts, no meaningful isotopic spallation composition could be derived for ALSH183 (backward recoil nuclei of the 330 MeV irradiation).

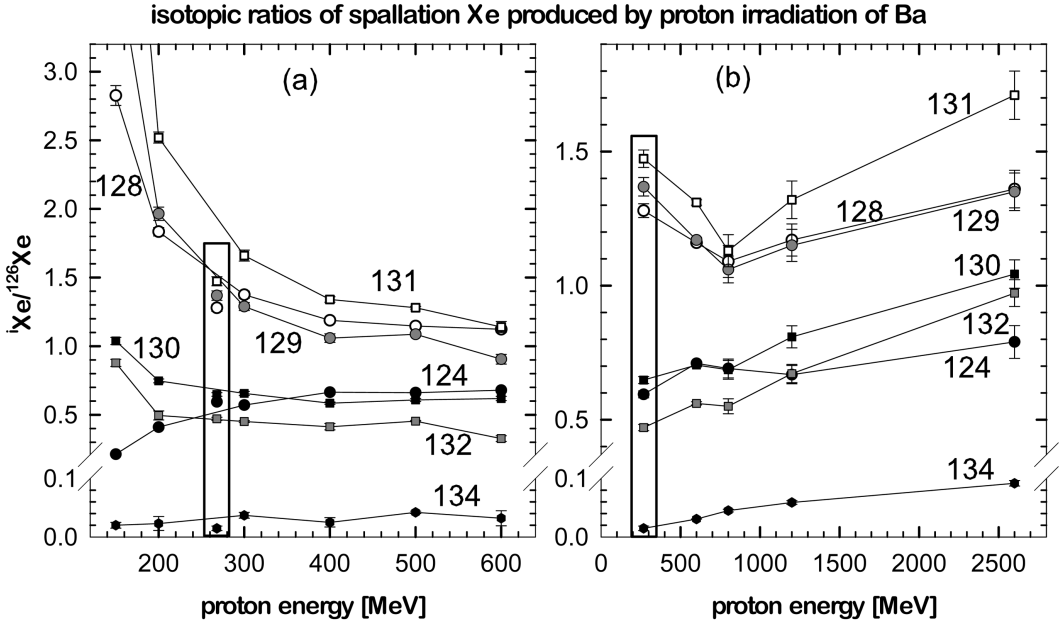

Fig. 2. Isotopic ratios of Xe produced by proton irradiation of Ba targets as a function of energy (normalizing isotope ^{126}Xe). On the left, our data for the 330 MeV irradiation (268 MeV at the target) are compared with those obtained by Kaiser (1977) at energies up to 600 MeV. The Kaiser data points are connected by lines, data from this work shown in box. On the right, our data (in box) are compared to ratios for higher energies from Mathew et al. (1994).

particle ejection from the intermediate nucleus. The equations of Sugarman et al. (1956) are strictly applicable only in case where the reaction leads to fissioning of the intermediate nucleus and where additional fission energy contributes to the recoil of nuclei ejected in the second step. Under these conditions momentum transfer from the impacting protons to the intermediate excited nucleus and further "inherited" by the recoiling nucleus of interest is small compared to the momentum acquired by the recoiling nucleus in the following fission process; the ratio of forward to backward recoils F/B is close to one. A further important assumption in the Sugarman et al. (1956) description, which is valid in the range of recoil energies considered by these authors, is that the range of recoil nuclei is proportional to their recoil energy.

The situation is different in the case of the true spallation reactions of interest here, where F/B >>1. Consequently, although the results do not differ by much, we have, following the suggestion of an anonymous reviewer, redone our calculations using the more generally applicable approach of Lagarde-Simonoff et al. (1976). Equations 4 and 4a of these authors give the numbers of forward (F) and backward (B) recoils, respectively, as a function of range R, target thickness W and three additional parameters: a) η, which in their formalism is the ratio v/V (v = velocity transferred to the intermediate nucleus; V = additional velocity of recoiling nucleus acquired during breakup of intermediate nucleus); b) N = the exponent in the range-velocity relation $R = K \times V^N$; and c) the anisotropy parameter b/a. For the calculation, we followed Lagarde-Simonoff et al. (1976) in assuming $b/a = 0$. With this assumption, their Equation 4 for the forward fraction F simplifies to:

$$F = [R/(16\eta^4 \times W)] \times \{(1+\eta)^{(N+1)}[(4\eta^2) \times (1+\eta)^2/(N+3) + (4\eta^2) \times (\eta^2-1)/(N+1)] - (1-\eta^2)^{1/2(N+1)}[(4\eta^2) \times (1-\eta^2)/(N+3) + (4\eta^2) \times (\eta^2-1)/(N+1)]\} \quad (4)$$

Similarly, their Equation 4a for the backward fraction B is obtained by changing η to −η.

For our calculations N for the relevant energy range was obtained from the range-energy relations of Ziegler et al. (2003). Then, as in Lagarde-Simonoff et al. (1976), η as well as the resulting ratio of recoil range to target thickness, was determined by varying η in the range 0 to 1 until the predicted ratio $Q_{cal} = 2(F + B)/(F - B)$ matched the observed one. Recoil ranges determined in this way are shorter than those calculated using the Sugarman et al. (1956) formalism. Differences are small, however (3–8% for the 1200 MeV experiment; between 11 and 14% for the 330 MeV experiment). They are much smaller than other uncertainties involved in determining a presolar cosmic ray exposure age, and they are inconsequential as far as our conclusions below are concerned.

Xe^{126} from 330 MeV and 1200 MeV Irradiations

Details of the recoil range calculations are given in

Table 5. Calculation parameters and inferred recoil ranges R (μm) for stable Xe isotopes in Ba glass and in SiC.

	^{124}Xe	^{126}Xe	^{128}Xe	^{129}Xe	^{130}Xe	^{131}Xe	^{132}Xe
N[a]	1.91	1.91	1.82	1.74	1.64	1.64	1.55
Proton energy 268 MeV[b]							
F	8.49×10^{-5}	6.85×10^{-5}	4.72×10^{-5}	–	–	–	–
B	2.07×10^{-6}	2.06×10^{-6}	1.93×10^{-6}	–	–	–	–
η[c]	0.61	0.59	0.56	–	–	–	–
R (Ba glass)	0.316 (39)	0.266 (25)	0.198 (54)	–	–	–	–
R (SiC)	0.260 (32)	0.219 (21)	0.164 (45)	–	–	–	–
Proton energy 1190 MeV[b]							
F	4.84×10^{-5}	3.72×10^{-5}	2.77×10^{-5}	2.56×10^{-5}	1.31×10^{-5}	1.79×10^{-5}	9.26×10^{-6}
B	3.62×10^{-6}	3.28×10^{-6}	2.81×10^{-6}	1.91×10^{-6}	2.27×10^{-6}	1.44×10^{-6}	1.56×10^{-6}
η[c]	0.46	0.43	0.42	0.48	0.35	0.47	0.36
R (Ba glass)	0.234 (20)	0.192 (15)	0.147 (13)	0.126 (16)	0.083 (11)	0.092 (12)	0.058 (17)
R (SiC)	0.194 (17)	0.159 (13)	0.123 (11)	0.106 (14)	0.070 (9)	0.078 (10)	0.050 (14)
R (SiC)-preferred	0.230 (58)	0.189 (44)	0.146 (37)	0.126 (34)	0.083 (19)	0.092 (22)	0.059 (22)

[a]Exponent N in range velocity relation $R = K \times V^N$.
[b]Actual proton energy at target position.
[c]Ratio of recoil velocity transferred to intermediate nucleus relative to velocity transferred during actual recoil.
Ranges have been calculated according to approach of Lagarde-Simonoff et al. (1976) as described in the text. *F* and *B* are the fractions of recoil atoms emitted in forward and backward directions, respectively.

Table 5. The targets are thick (3.25 mm) compared to the recoil range of spallogenic Xe, so losses are negligible compared to the inventory in the target and the measured concentrations in the target material properly reflect production. For the 330 MeV irradiation, the amounts of ^{126}Xe found in the forward and backward catcher foils correspond to 6.8×10^{-5}, and 2.1×10^{-6} times, respectively, those in the Ba glass target (Tables 3 and 4). This translates into a recoil range in Ba glass of (0.266 ± 0.025) μm. Using range-energy relations according to the SRIM code (Ziegler 2003), this corresponds to a mean energy of the recoiling ^{126}Xe nuclei of ~860 keV, and to a corresponding range in silicon carbide of (0.219 ± 0.021) μm. This is more than a factor of 2 shorter than the 0.5 μm recoil range extrapolated by Ott and Begemann (2000) based on the data by Lagarde-Simonoff et al. (1976) for recoils in the Sc to Cu region. Consequently, retention of spallation Xe is even larger than shown in their Fig. 7, where they show retention as a function of recoil ranges between 0.3 and 0.7 μm.

Recoil ranges calculated in the same manner from the 1200 MeV irradiation are shorter, (0.192 ± 0.015) for ^{126}Xe in the Ba glass, equivalent to (0.159 ± 0.013) μm in SiC. This is somewhat unexpected, since recoil ranges are thought to be largely independent of the energy of the primary protons (Ott and Begemann 2000). It is also counterintuitive, since, if anything, the naive expectation would be to have larger losses at higher, not lower energy. A major difference is also not supported by the observations on spallation Na and Ne discussed below. One possible reason for a difference is interlaboratory bias, since the 1200 MeV target was analyzed in a different laboratory (PRL) (Mathew et al. 1994). In the case of the 330 MeV experiment this source of error does not exist, since the Xe in catchers and target were measured on the same mass spectrometer and because to calculate ranges only ratios of abundances are needed.

On the other hand, the difference seems too large for blaming it entirely on interlaboratory bias, and a small difference between recoil ranges at the two energies is a possibility that needs to be considered. While the fraction of recoils *F* in forward direction in the lower energy experiment is higher than at the higher energy, the fraction *B* emitted backwards is lower, and the ratio *F*/*B* is distinctly higher (~33 versus ~11). This observation indicates that more momentum is transferred to the intermediate excited nucleus from 330 MeV protons than from 1200 MeV protons, in spite of the smaller available energy. Accordingly, less momentum must be transferred to promptly emitted light particles, i.e., the nuclear mechanisms at the two energies differ in detail.

Because of this, and because most of the production of cosmic ray spallation Xe is within the energy range bounded by the energies of the two experiments, we feel that an average of the two ranges is a reasonable best choice for our discussion of recoil losses and ages below. Preferred values for ^{126}Xe were obtained d by averaging the ranges from both experiments; ranges for the other isotopes (not of all which are available from the 330 MeV experiment) from the 1200 MeV irradiation were scaled in proportion. They are listed in the bottom line of Table 5. As discussed in the Uncertainties section, the exact choice is not critical for our conclusions. An error has been assigned to the preferred ^{126}Xe range based on the variation between the two experiments. For the other isotopes, this error was quadratically added with the individual error of the range determined at 1200 MeV.

Isotopic Compositions

In addition to the short recoil range of spallogenic Xe, we

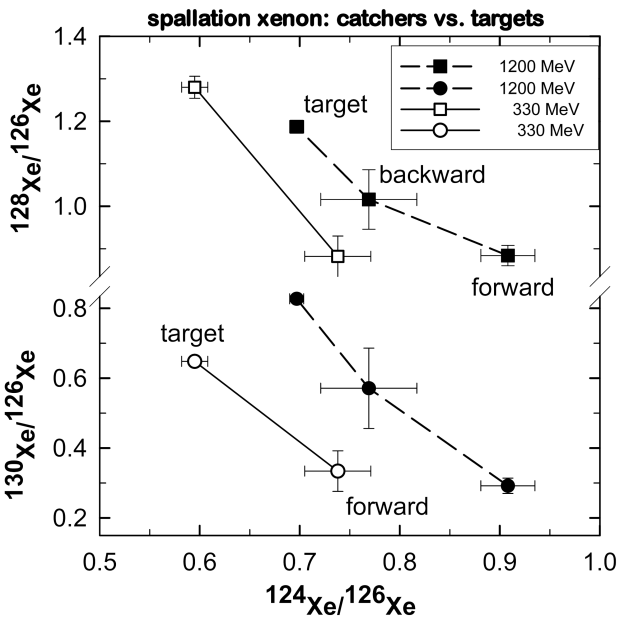

Fig. 3. Spallation Xe isotopic ratios in targets and catcher foils. For the 1200 MeV irradiation target (Mathew et al. 1994), both forward and backward catcher foils are plotted, while for the 330 MeV irradiation, only target and forward catcher foil are plotted (Tables 3 and 4).

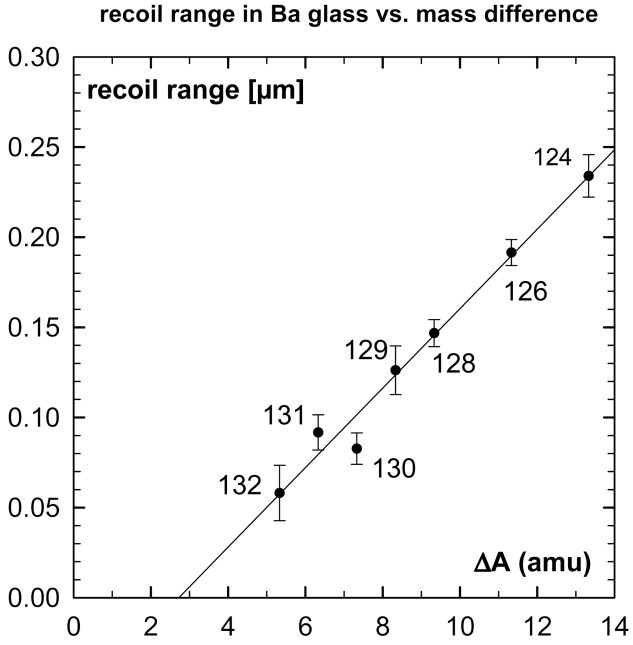

Fig. 4. Plot of recoil range (Table 5) for various Xe isotopes produced in Ba glass (composition given in Table 1) versus mass difference (Ba atomic weight = 137.33 amu).

observe a difference in isotopic composition between spallation Xe in the target (i.e., as produced, given the small relative loss <0.01%) and recoil Xe in the catchers (Tables 3 and 4). This is illustrated in Fig. 3, which is a 3-isotope plot of spallation $^{128}Xe/^{126}Xe$ and $^{130}Xe/^{126}Xe$, respectively versus the $^{124}Xe/^{126}Xe$ ratio. The recoil ranges of different isotopes differ, scaling approximately linearly with A, the mass difference between target (Ba) and the product nucleus (Fig. 4). This behavior has been seen also in other studies of recoil nuclei in spallation (e.g., Lagarde-Simonoff et al. 1976). Inferred mean recoil energies for the 1200 MeV irradiation range between ~0.16 MeV for ^{132}Xe and ~0.76 MeV for ^{124}Xe.

In the case of our thick target experiments, differential recoil release does not noticeably affect the ratios in the target itself and also not the relative retentions. There are significant losses in the case of small grains, however. Accordingly, in the following discussion recoil loss corrections will be applied individually to each isotope.

Low-Energy Recoil (71 MeV Irradiation)

Xe-127: Because we have only upper limits for the ^{127}Xe activity in the catcher foils, the results are of limited value. A maximum upper limit (in Ba glass) is 5.3 μm, which corresponds to F/B (ratio of forward to backward recoils) being close to unity. Under these conditions, the parameter η in the Lagarde et al. (1977) formulism is close to zero, i.e., this is the situation that is approached in induced fission reactions, but not in true spallation (see Calculation of Recoil Ranges section). Assuming a more reasonable value of F/B, similar to those in the 300 and 1200 MeV irradiations, an upper limit of ~2 μm is implied, but even this is likely to exceed the true value by a large factor.

Na-22 : Here the situation is more favorable. Our data in Table 2 indicate a recoil range of ^{22}Na in Ba glass of (2.00 ± 0.58) μm or (1.55 ± 0.46) μm in SiC. This is clearly compatible with data obtained at higher energies, such as in the experiments of Steinberg and Winsberg (1974). These authors determined recoil of spallation ^{22}Na—produced by protons in the energy range 3,000 to 30,000 MeV—in Al and found a range of 2.3 μm (2.2. μm, if recalculated with the Lagarde-Simonoff formalism). This is virtually identical with the ~2.1 μm range in Al that is implied by our low energy data for the Ba glass. Notwithstanding small variations as discussed above (see Xe^{126} from 330 MeV and 1200 MeV Irradiations section), these results support the conclusion that there is no significant variation in recoil range with energy of the primary projectile, over the relevant energy range where most of the production occurs.

DISCUSSION

Recoil Losses

We have calculated the recoil losses of ^{124}Xe, ^{126}Xe, ^{128}Xe, and ^{130}Xe as a function of grain size using the "preferred" recoil ranges of Table 5. The results are shown in

Fig. 5, where two sets of curves are shown: a) a set using a straggling in the recoil range of 15%, which is typical for the longitudinal range straggling for Xe ions of the implied energies (Ziegler 2003); and b) a second set of curves that assumes 40% straggling. The latter case is meant to include, apart from "true straggling" in range, variations due to variability in recoil energy. It is also meant to mimic, in addition, the effect of having, in the real (meteoritic) case, a distribution of sizes and shapes around the mean spherical diameter plotted on the abscissa.

Two properties of the curves are remarkable. First, they show that over the whole size range of the presolar silicon carbide grains in meteorites (mostly in the range 0.3–5 μm; Amari et al. 1994) retention of spallation Xe is finite. For a "typical" 1 μm grain, e.g., ^{126}Xe retention is ~70%. This is in stark contrast to spallation Ne, which from grains smaller than ~3 μm is almost quantitatively lost (Ott and Begemann 2000; Fig. 5). Additionally, over much of the smaller size range (<1 μm) retention differs quite significantly for the different spallogenic Xe isotopes. For a 0.5 μm grain, for example, retention of ^{124}Xe is barely half that of ^{130}Xe.

The latter effect makes it difficult to infer the amount of spallation Xe present from three-isotope diagrams based on the deviation from mixing lines between other components known or expected to be present. Instead, in the following section we will first concentrate on the inverse approach, i.e., investigate the effect of an assumed cosmic ray exposure on the position of data points.

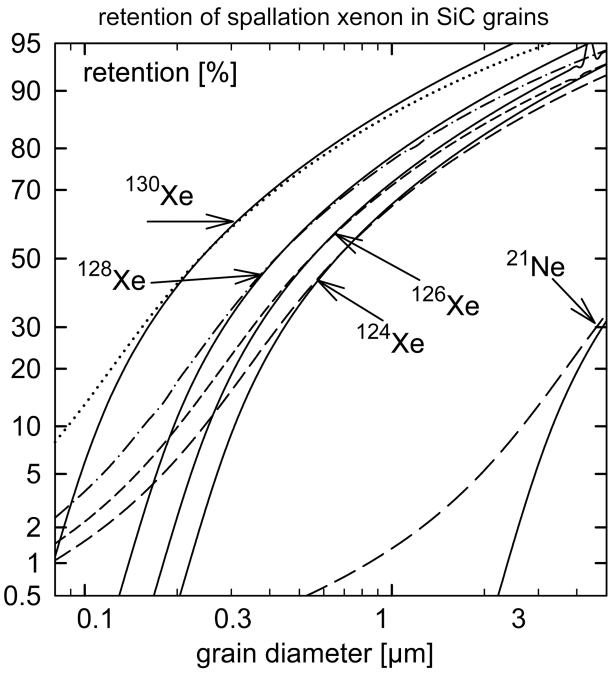

Fig. 5. Retention of spallation ^{124,126,128,130}Xe produced on Ba in SiC inferred from the recoil ranges listed in Table 5. Two sets of curves are shown: one including 15% longitudinal range straggling (full lines), the other assuming 40% straggling (dashed/dotted lines). See text for discussion. Also shown are the equivalent curves for ^{21}Ne produced on SiC, based on a ~2.5 μm recoil range (Ott and Begemann 2000).

Age and History of Presolar SiC

In this section, we investigate the effect of cosmogenic Xe on the Xe data for the KJ size separates reported by Lewis et al. (1994). Because the situation is complex, and it is difficult to extract exact amounts and compositions of spallation Xe from the measured data, we are first taking the inverse approach: we assume a spread of cosmic ray exposure ages, determine the effect that subtraction of the corresponding spallation Xe would have on the Xe isotopic composition and compare the residuals with known trapped Xe components.

Trapped xenon in presolar SiC consists of two major components mixed in about equal parts (Lewis et al. 1994). One (Xe-G) corresponds to Xe manufactured by the s-process in the region between the H- and He-burning shells of asymptotic giant branch (AGB) stars as well as in the He-burning shell itself (cf. Straniero et al. 1997). The other, isotopically more normal component (Xe-N) presumably derives from the envelope of those AGB stars. We have argued before (Ott and Begemann 2000), based on the position of data points in a ^{126}Xe/^{132}Xe versus ^{136}Xe/^{132}Xe plot, that there is evidence for the presence of spallation Xe. However, arguments involving the heavy isotopes are not straightforward, since Lewis et al. (1994) have shown that Xe-N shows enhanced abundances of ^{134}Xe and ^{136}Xe. In order to be on safer ground, we here consider only the light Xe isotopes 124, 126, 128, and 130, which not only seem to occur in rather normal relative abundances in Xe-N (Lewis et al. 1994), but which are also most sensitive to addition of spallation products.

Production and Loss of Spallation Xe

In order to explore expected amounts and isotopic compositions of spallation Xe for a given grain ensemble as a function of cosmic ray exposure, two quantities have to be known: production rates and extent of recoil losses. Relevant inferred input parameters for both are listed in Table 6 and are discussed in detail below.

Production on Ba by GCR Protons

Because this is the most important mechanism, relevant cross-sections have been obtained by a number of workers (see Cross-Sections section). In spite of the fact that results not always are consistent, the largest source of error lies in the uncertainty of flux and energy distribution of cosmic ray protons in the relevant regions of interstellar space. For the calculation, we follow Reedy (1989), who investigated production rates for ^{21}Ne in presolar SiC grains: we consider

Table 6. Inferred production and retention of spallation Xe in presolar SiC grains analyzed for noble gases by Lewis et al. (1994).

Sample[a]	KJA	KJB	KJC	KJD	KJE	KJF
Size (μm)[a]	0.38	0.49	0.67	0.81	1.14	1.86
Ba (ppm)[b]	442	243	163	148	164	129
La (ppm)[b]	18	27	19	19	19	17
Ce (ppm)[b]	48	76	54	57	62	46
P_{126}[c]	2.638	1.867	1.274	1.200	1.279	1.056
P_{126}(loss-corr)[c]	0.821	0.741	0.676	0.719	0.907	0.858
$^{124}Xe/^{126}Xe$	0.624	0.657	0.659	0.663	0.658	0.664
Loss-corrected	0.449	0.506	0.555	0.580	0.605	0.634
$^{128}Xe/^{126}Xe$	1.270	1.259	1.258	1.257	1.258	1.256
Loss-corrected	1.737	1.582	1.461	1.412	1.356	1.310
$^{130}Xe/^{126}Xe$	0.547	0.434	0.427	0.413	0.428	0.409
Loss-corrected	1.173	0.799	0.642	0.572	0.529	0.463

[a]Names and sizes from Amari et al. (1994) and Lewis et al. (1994).

[b]Ba and REE abundances from Zinner et al. (1991) and Zinner (personal communication); abundances of Nd and Sm are in the range 25–39 and 1.29–1.84 ppm, respectively (Zinner et al. 1991).

[c]Production rates in units of 10^{-12} cm^3 STP g^{-1} Ma^{-1}.

Production rates (see text for details of calculation) and rates of retained spallation ^{126}Xe as well as isotopic ratios before and after correction for recoil loss for presolar SiC grain size separates analyzed by Lewis et al. (1994).

various possible spectra as shown in detail in Reedy (1987), calculate the according production rates for ^{126}Xe, and take a geometric mean of these. In detail these are the spectra as given by Castagnoli and Lal (1980) with M = 0; by Webber and Yushak (1983); and by Ip and Axford (1985). We do not use the fourth spectrum considered by Reedy (1989), which is an estimate for the GCR source. Cross-sections were taken from Prescher et al. (1991) for proton energies up to 30 MeV, and interpolated/mean values derived from Kaiser (1977), Mathew et al. (1994), Gilabert et al. (1997), and this work, at higher energies. Production rates for ^{126}Xe based on the three spectra vary between 2.2×10^{-15} and 7.2×10^{-15} cm^3 STP (ppm Ba)$^{-1}$ (Ma)$^{-1}$, with a geometric mean of 3.74×10^{-15}. Inclusion of the fourth spectrum considered by Reedy (1989) would raise the mean to 4.34×10^{-15}. In all cases most of the production (>90%) is by protons in the 0.1 to 3 GeV range, and peaks between 0.3 and 1 GeV.

Contribution by GCR α-particles

Cross-sections for reactions induced by galactic cosmic ray α-particles are rare (e.g., Lange et al. 1995), and, for heavy elements like Ba and rare earth elements (REE) non-existent. With galactic cosmic rays consisting of ~87% protons and 12% α-particles (Simpson 1983), models for production of cosmogenic nuclides in stony meteorites (e.g., Michel et al. 1991; Leya et al. 2000) usually take α-particles into account by multiplying the proton-induced rate by a scaling factor of 1.55. This is based on the assumption that incoming α-particles break up into four nucleons in the first inelastic collision, and then behave essentially just as four protons would. This reasoning, of course, does not apply in the case of ~μm-sized presolar grains, where reactions are dominated by primary particles. Reedy (1989) has explicitly modeled the production by α-particles of Li from O, and of Li and B from C. In his assessment, ~10% of the production is by α-particles in the former case, ~25% in the latter, equivalent to scaling factors 1.11 and 1.33, respectively. Comparison of p- and α-rates for a variety of light target-product combinations (taken from Bodemann et al. 1993 and Lange et al. 1995) shows α-rates to be clearly higher than p-rates (as expected), but quite substantial variations among different target-product combinations. For our application, we have chosen a mean scaling factor of 1.33, which corresponds to a cross-section enhancement $\sigma(\alpha)/\sigma(p)$ ~2.5, i.e., approximately the ratio of the geometrical cross-sections. Reactions induced by the heavier nuclei in the GCR are neglected, as is usual in such studies (e.g., Leya et al. 2000).

Production from REE

Unfortunately, again, there is little hard information on relevant nuclear cross-sections. We therefore follow the empirical relationship of Eugster (1988) for chondritic meteorites, according to which P_{REE} = (6076/1239) * ([La] / [Ba]) * P_{Ba}, i.e., the production from REE is 4.9 times production from Ba multiplied with the La/Ba elemental ratio. The applicability of the equation depends on the REE abundance pattern (assumed to be chondritic), primarily the relative abundances of the lightest REEs. For the average abundances in the SiC grain size separates of Lewis et al. (1994), to which we will apply the formalism, this appears to be roughly the case (Table 6). Application of the Hohenberg et al. (1981) empirical formula, which takes into account abundances of La, Ce and Nd, provides essentially identical results. Among the REEs (Table 6; data from Zinner et al. 1991; and Zinner 1994, personal communication), Ce is the most important target. Production on REEs adds between ~20% and 40% overall to the production of spallogenic ^{126}Xe (Table 6).

Isotopic Composition of Spallation Xe

The isotopic composition of Xe produced on Ba varies strongly at low energies, but in the energy range 0.1–3 GeV, where >90% spallation Xe is produced, there are only moderate variations (Fig. 2). We use the composition obtained in our 330 MeV irradiation experiment, which represents a rather typical average value. For Xe produced on REEs, we use the composition inferred by Hohenberg et al. (1981).

Recoil Losses

Determining the recoil losses of spallation Xe produced on Ba, which is the main target element, has been the central issue of this work. We apply retention factors based on the "preferred" recoil ranges in SiC listed in Table 5 and assuming 40% range straggling as in Fig. 5. As the recoil range scales with mass difference between target and residual nucleus (Fig. 4), we treat nuclei produced by spallation on REE separately. We extrapolate the range-mass difference relation shown in Fig. 4 to the appropriate mass difference, using 141.0 (approximate weighted average of La, Ce, Nd, and Sm in the abundance ratios listed in Table 6) as the average REE mass for production of spallation Xe and calculate resulting recoil ranges and retention. The final results, "recoil corrected" production rates and isotopic ratios are also given in Table 6.

Cosmic Ray Ages: Nominal Values, Upper Limits, and Occam's Razor

As pointed out in the introduction to the Age and History of Presolar SiC section, we will first approach the problem by a) assuming a spread of cosmic ray exposure ages; b) then determining the effect that subtraction of the corresponding spallation Xe (produced and retained as described in the Production and Loss of Spallation Xe section and with the input parameters from Table 6) would have on the Xe isotopic composition; and c) finally comparing the "spallation-corrected" residuals with known trapped Xe components. Because of complexities in the heavy Xe isotopes (Lewis et al. 1994; see also discussion of Xe-N component in SiC by Pepin et al. 1995; and further arguments below), we consider only the light isotopes 124, 126, 128, and 130, which are also the ones that are most affected by spallation contributions.

Results from this approach are shown in the three-isotope diagrams of Figs. 6 and 7. In both diagrams the ratios for grain size separates KJA to KJF as reported by Lewis et al. (1994) are shown with errors bars; lines extending from these measured data points (towards the lower left in Figs. 6a and 6b; towards the upper right in Fig. 7) show the effect of subtracting spallation contributions. These lines define the composition of the trapped component for a given cosmic ray exposure age. Since the trapped component itself is a mixture of s-process produced "Xe-G" and approximately normal "Xe-N" (Lewis et al. 1994), and since the composition of Xe-G is well established (Lewis et al. 1990, 1994; Gallino et al. 1990), the lines in effect put constraints on the Xe-N composition and the G/N mixing ratio. Results after subtracting spallation Xe produced by 100 Ma irradiation are shown by blue symbols, those for 200 and 300 Ma irradiation in green and red, respectively. In addition, labels A to D mark the effect of subtracting for a 300 Ma exposure from KJA to KJD (KJE and KJF being off scale). Differences in slope are due to differences in spallation Xe composition (Table 6) caused by the different retention and (to lesser extent) differences in the Ba/REE ratio. Also shown are mixing lines between Xe-G (Lewis et al. 1994) and both, Q-Xe (=Xe-P1) and Xe-HL (Huss and Lewis 1994; Huss et al. 1996; Busemann et al. 2000; Ott 2002).

An important observation in these diagrams is that the measured data points all lie very close to the Xe-G $\leftarrow \rightarrow$ Q-Xe mixing line. If Q-Xe is the dominant trapped component besides Xe-G, there clearly is not much room for additional contributions from spallation, or anything else. This is especially so for KJE and KJF, which because of their low trapped Xe contents are most susceptible to the presence of additional Xe components. Of course, there has to be at least some spallation Xe, since the presolar SiC grains on their way towards the solar-system-to-be cannot have avoided being exposed to cosmic rays. The products of the recent irradiation within the Murchison meteorite, which is on the order of 1 Ma, much shorter than the time scales we are looking for, are of no consequence.

In Figs. 6a and 7, the situation is simpler than that shown in Fig. 6b. In the latter, where $^{128}Xe/^{130}Xe$ is plotted versus $^{126}Xe/^{130}Xe$, measurements, excepting KJF, plot to the lower right of the G-Q mixing line. However, deviations in $^{128}Xe/^{130}Xe$ from the line are on the order of 1% only and thus may not be significant, given possible systematic uncertainties in the composition of the established components. It is clear, nevertheless, from both Figs. 6a and 6b that very long cosmic ray exposure ages require the trapped component to have a rather exotic composition. For nominal exposures of, e.g., more than 121 Ma for KJF and more than 184 Ma for KJE, all ^{126}Xe present is required to be of cosmogenic origin, leaving no ^{126}Xe at all for the trapped Xe-N component - a conclusion that is hard to believe. Fig. 7 displays a different view of the data set. Since ^{124}Xe and ^{126}Xe are not made by the s-process, variable amounts of s-process-Xe (Xe-G) lead only to a horizontal shift in this diagram, not affecting the $^{124}Xe/^{126}Xe$ ratio that is plotted on the ordinate. Here data points plot at or slightly below the $^{124}Xe/^{126}Xe$ ratio for Q-Xe, which, again, is remarkable since these are the two isotopes most strongly affected by the addition of spallation Xe. Again, this demonstrates that there is not much room for cosmogenic Xe. In addition, the data suggest the trapped component may have a $^{124}Xe/^{126}Xe$ ratio lower than that in Q.

In a second, more direct approach, we have also calculated nominal amounts of cosmogenic ^{126}Xe via the

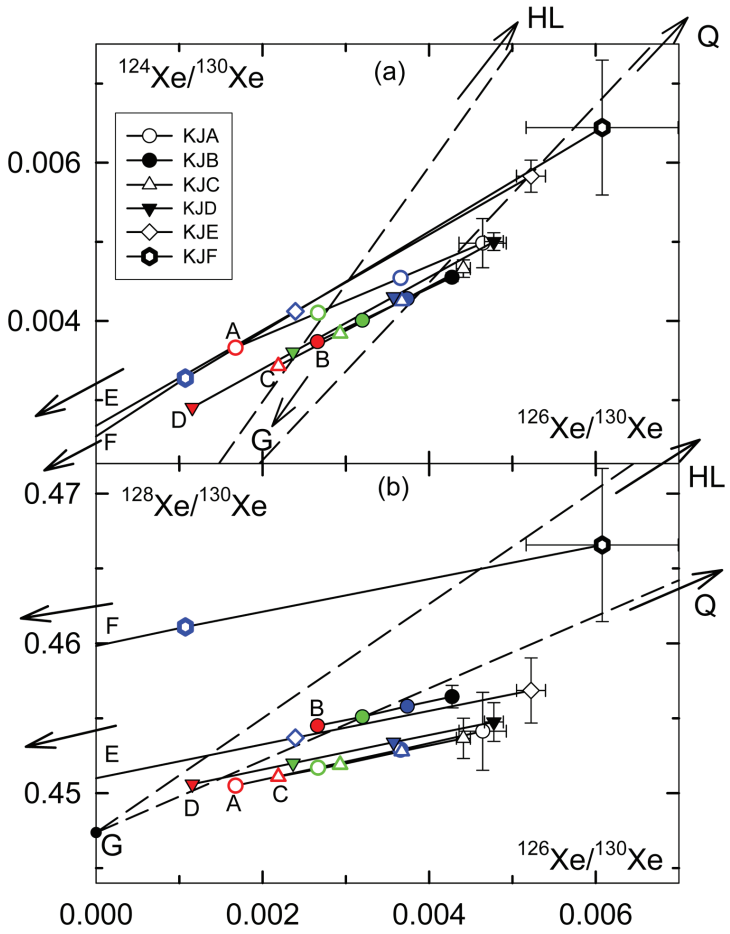

Fig. 6. Effects of spallation on Xe isotopic composition. Top: three-isotope plot ^{124}Xe/^{130}Xe versus ^{126}Xe/^{130}Xe. Bottom: ^{128}Xe/^{130}Xe versus ^{126}Xe/^{130}Xe. Shown with error bars are the isotopic compositions measured by Lewis et al. (1994). Subtraction of spallation Xe with the compositions listed in Table 6 leads to inferred trapped compositions along the lines (blue 100 Ma; green 200 Ma; red 300 Ma). In addition, labels A to D mark the effect of subtracting a 300 Ma irradiation on KJA to KJD. For KJE and KJF the lines pass trough ^{126}Xe/^{130}Xe=0 (meaning all ^{126}Xe being cosmogenic) for exposure ages of 184 and 121 Ma, respectively (see text). Also shown are mixing lines between s-process Xe (= Xe-G) and both Q-Xe and Xe-HL (e.g., Ott 2002).

^{124}Xe/^{126}Xe ratio, using various reasonable assumptions for ^{124}Xe/^{126}Xe in the trapped component, together with the recoil-corrected cosmogenic compositions given in Table 6. The resulting nominal exposure ages calculated using the "corrected" production rates in Table 6 are shown in Fig. 8a, where they are plotted versus the grain size of the Lewis et al. (1994) separates. Assuming the trapped composition to have the Q isotopic ratio, they range from ~2 and ~14 Ma for KJE and KJF, respectively, up to ~64 and ~68 Ma for KJC and KJB, respectively. Maximum spallation contributions—assuming for the measured ratio the value at the lower end of the analytical uncertainty range—lie between ~20 Ma for KJE and ~95 Ma for KJA in this case. They are slightly higher, if we assume the trapped component to have the ^{124}Xe/^{126}Xe ratio of U-Xe (identical to the ratio in the solar wind; Pepin et al. 1995; Wieler 2002). Alternatively, one may argue that trapped Xe in the SiC grains could have a ^{124}Xe/^{126}Xe ratio that is enhanced relative to the ratio in Q, in analogy to the enhanced ^{136}Xe/^{130}Xe ratio in the N component in presolar SiC (Lewis et al. 1994). If we assume addition of a HL-like component that is consistent with the heavy Xe isotope data (28% enhancement at ^{136}Xe, implying ~20% enhancement at ^{124}Xe and ~10% at ^{126}Xe), this would raise the "true trapped ^{124}Xe/^{126}Xe ratio" from the Q value of 1.12 to ~1.22 and allow for maximum (as defined above) exposure ages between ~45 Ma for KJE and ~175 Ma for KJB. There can be no doubt that, unless our assumptions are seriously flawed, exposure ages for the KJ series of presolar SiC grains are considerably shorter than theoretically expected lifetimes for interstellar grains (Jones et al. 1994, 1997).

True exposure ages may even be shorter than the "nominal" values calculated above. This is suggested by the fact that, for all these choices of trapped ^{124}Xe/^{126}Xe, apparent amounts of cosmogenic Xe as well as derived ages scale with the concentration of total ^{126}Xe—a possible consequence of overestimating ^{124}Xe/^{126}Xe in the trapped

component, even with the lowest value, i.e., the Q composition (Fig. 8b). This is further illustrated by the "low" case also plotted in Figs. 8a and 8b. Here a "low" value of 1.065 is assumed for trapped $^{124}Xe/^{126}Xe$, which is similar to the ratio measured by Lewis et al. (1994) for the most gas-rich and most precisely measured separate KJB. Remarkably, this is also the value where there is best agreement among nominal exposure ages for the various grain size separates, and where there is no apparent correlation with total ^{126}Xe concentration. And even more remarkably, all ages are compatible with zero for this choice. Of course, there is no a priori reason, why all size fractions should have the same average (short) exposure age, but Occam's razor would suggest the simplest explanation of all: a ratio of ~1.065 for trapped $^{124}Xe/^{126}Xe$, and spallation contributions that are negligible.

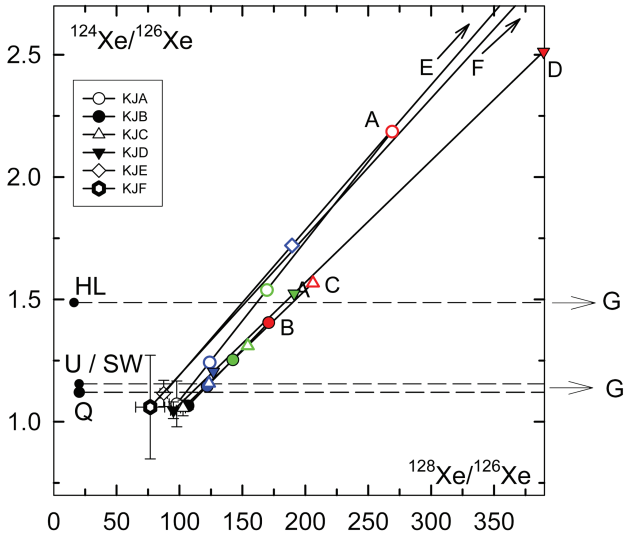

Fig 7. Effects of spallation on Xe isotopic composition in a three-isotope plot $^{124}Xe/^{126}Xe$ versus $^{128}Xe/^{126}Xe$. Shown with error bars are the isotopic compositions measured by Lewis et al. (1994). Subtraction of spallation Xe with the compositions listed in Table 6 leads to inferred trapped compositions along the lines (blue 100 Ma; green 200 Ma; red 300 Ma). In addition, labels A to D show the effect of subtracting a 300 Ma irradiation on KJA to KJD. Mixing lines between s-process Xe (= Xe-G) and Q-Xe/Xe-HL/U-Xe (the latter being virtually identical to solar wind in these ratios) (e.g., Ott 2002; Wieler 2002) are horizontal, because s-process Xe does not contain ^{124}Xe or ^{126}Xe.

Uncertainties

Our discussion of ^{126}Xe-based cosmic ray exposure ages for the Lewis et al. (1994) presolar SiC grains in the preceding chapter has been based on what we believe are reasonable choices for three critical parameters: ^{126}Xe production rate, isotopic composition of trapped xenon, and retention of spallation Xe.

Retention

Least critical, with the experimental results from our study, are the recoil losses, which we believe should introduce not more than about 25% uncertainty on ages (cf. Fig. 5). The principal effect of choosing another than the "preferred" (mean) value from the two experiments is to change the recoil-corrected ^{126}Xe production rate in Table 6. The effect is largest for KJA with the smallest grain size and accordingly highest recoil losses. KJA ages calculated relative to the trapped Q composition, e.g., using the nominal ranges obtained in the 330 and 1200 MeV experiments (Table 5) differ by about 20% from those obtained using the "preferred," i.e., average recoil ranges. For the other size separates the differences are much smaller. Clearly, recoil loss is not a major issue.

Production Rates

The relevant production rate in interstellar space (Production and Loss of Spallation Xe section) is uncertain primarily because of uncertainties concerning flux and energy spectrum of the cosmic rays. Following Reedy (1987, 1989) we have based our estimate on a mean obtained from considering three possible spectra. Individual production rates calculated based on these spectra differ by about a factor of 3. Reedy (1987, 1989), in taking the same approach in calculating production rates by primary cosmic ray protons of light nuclei including ^{21}Ne, estimates the uncertainty due to the spread in fluxes as a factor ~2. The situation for spallation Xe is actually somewhat more favorable than for ^{21}Ne, because only little of the production is due to low-energy cosmic rays below 100 MeV (cf. cross-sections in Fig. 1, and, e.g., those for ^{21}Ne on Si in Walton et al. 1976); as a consequence differences in inferred production rates are mostly caused by differences in absolute flux rather than by differences in the energy spectra. Following Reedy (1987, 1989) we estimate the mean production rate used here also to be correct within about a factor of 2, provided most of the irradiation indeed occurred in an environment similar to the current local interstellar medium. Although more uncertain than recoil loss, a factor of 2 uncertainty in production rates will not change the main conclusion, i.e., exposure ages being short compared to expected lifetimes of interstellar grains.

Trapped Xe

Most critical is the assumption of a composition for trapped xenon. We have based our estimates for possible ages primarily on the $^{124}Xe/^{126}Xe$ ratio (Figs. 7 and 8; Cosmic Ray Ages: Nominal Values, Upper Limits, and Occam's Razor section). The primary reason, as stated there, is that—with these two isotopes absent from Xe-G of s-process origin—of all possible ratios this is the most likely to conform to a simple binary mixing relation between a single trapped component (Xe-N) (Lewis et al. 1994) and the spallation component. As shown in Fig. 7, the most remarkable fact about this ratio is

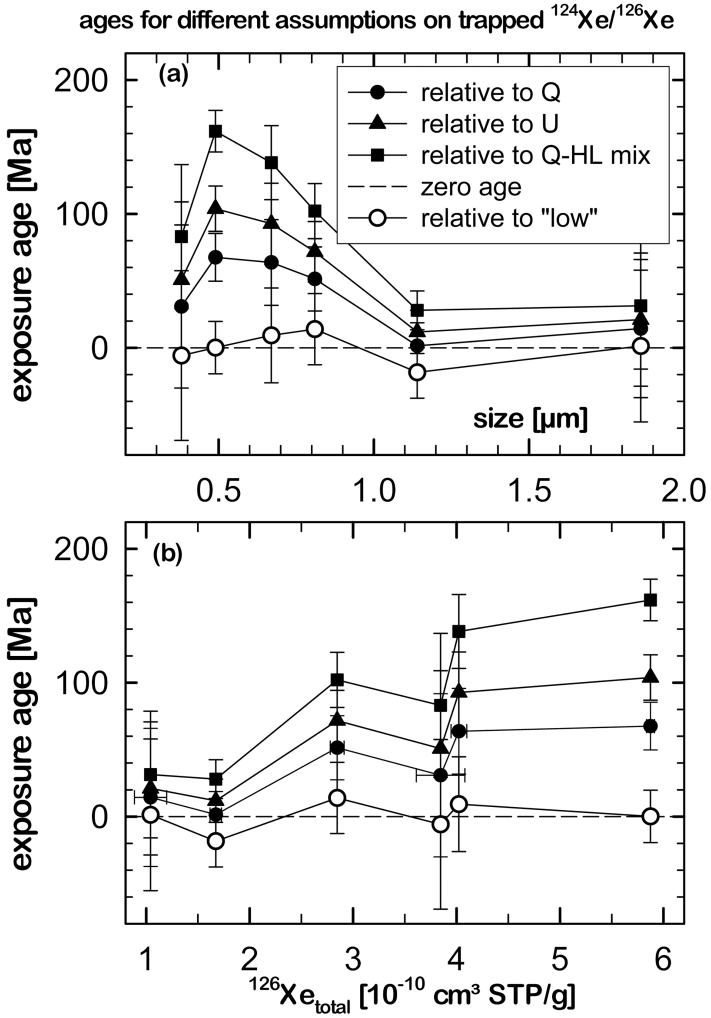

Fig. 8. a) Nominal exposure ages for presolar SiC based on apparent cosmogenic ^{126}Xe versus grain size of SiC separates. Four curves are shown for four different choices of trapped ^{124}Xe/^{126}Xe for dividing ^{126}Xe between trapped and cosmogenic components: 1) as in Q-Xe; 2) as in U-Xe (identical to the ratio in solar wind Xe); 3) a mixture of Q and HL-Xe based on the observed enhanced ^{136}Xe/^{130}Xe ratio (see text); and 4) for a "low" ^{124}Xe/^{126}Xe ratio of 1.065, similar to the ratio in the most gas-rich separate, KJB (Lewis et al. 1994). Cosmogenic ^{124}Xe/^{126}Xe used in the calculation of the cosmogenic ^{126}Xe abundances and production rates for the individual size separates as given in Table 6. b) Nominal exposure ages plotted versus concentration of total ^{126}Xe rather than grain size in the KJ separates of Lewis et al. (1994).

that it is, within analytical uncertainties, identical for all grain size separates from KJA to KJF. This is hardly to be expected, if there is a significant contribution from spallation, since the importance of the spallation component should increase with decreasing concentration of trapped Xe. Of course, there is no a priori reason why all separates should have the same average exposure age and several effects may have conspired so that they ended up with the same ratio. However, as discussed above, one possible interpretation and, following Occam's razor, the most likely is that spallation contributions are negligible and that ^{124}Xe/^{126}Xe ~1.07 simply is characteristic for the "normal" Xe-N component in presolar SiC. But also with the higher ratios discussed in the Cosmic Ray Ages: Nominal Values, Upper Limits, and Occam's Razor section, nominal ages are clearly shorter than the expected lifetime of interstellar grains, even when including possible uncertainties in recoil loss and production rate as discussed above.

Short (and/or Protected) Life of Presolar SiC

The principal result from our consideration of possible cosmic ray exposure ages can be summarized by stating that none of the SiC separates requires the presence of any spallation Xe and that the large majority of SiC grains may have formed rather shortly before entering into what was to become the solar system. There are two independent supporting observations that also indicate a short residence time of presolar SiC grains in the interstellar medium: their fresh appearance and the grain size distribution.

Fresh Appearance

Using scanning electron microscopy, Bernatowicz et al. (2003) studied "pristine" SiC grains that were extracted from the Murchison meteorite in their original state, i.e., without the use of chemicals. They found little to no evidence in the appearance of the grains for the processes thought to have occurred in the interstellar medium and thought to have left their imprint: grain-grain collisions induced by supernova shock waves and leading to comminution, as well as surface sputtering from collision with gas and cratering by collision with smaller particles. They point out (but find unlikely) a "facile" solution to the problem: only a subset of grains that were unprocessed in the interstellar medium survived incorporation into the solar system, while others were comminuted to very small grain sizes or entirely destroyed. The "unprocessed" grains would, of course, likely be young, so this would also be a "facile" solution to the problem of young cosmic ray exposure ages.

It may be premature to reject such a "facile solution" outright. Recent observations by Kemper et al. (2004) by infrared spectroscopy, using the Infrared Space Observatory (ISO), show that silicates in the diffuse interstellar medium are largely amorphous, with crystalline silicates accounting for only (0.2 ± 0.2)% by mass. The interpretation of Kemper et al. is that for silicates an amorphization process occurs in the ISM on a time scale on the order of ~5 Ma only, significantly shorter than the destruction time scale. There is no reason to suspect the situation for SiC to be fundamentally different. Hence, given the fact that amorphous SiC may be less resistant to conditions in the early solar nebula than the crystalline SiC that Mendybaev et al. (2002) considered, it may indeed be only relatively unprocessed young material that survived formation of the solar system and incorporation into primitive meteorites.

Grain Sizes

If so, the grain size distribution of the observed SiC should reflect the distribution established during condensation in the winds of AGB stars. As established by Amari et al. (1994), grain sizes for the KJ series of SiC grains can be described by either a log-normal distribution, or a power law $N = C \times a^{-b}$, with N = number of grains, a = diameter, parameter b = 5.7 in the incremental distribution, truncated at 0.6 μm and 3.2 μm at the lower and upper end, respectively. The slope differs significantly from that of the commonly used MRN distribution (Mathis et al. 1977), which describes the size distribution of interstellar grains in the size range 0.025 to 0.25 μm and which, by necessity, must include the effects of processing in the interstellar medium. It has been noted (e.g., Whittet 2003) that the sharp cut-off in the NRM distribution at larger sizes is unphysical and that a better description may be given by a distribution of the form $n(a) \propto a^{-3.5} \exp(-a/a_0)$, where the additional factor $\exp(-a/a_0)$ avoids this cutoff, and where the parameter a_0 defines the typical size of the large grains. In fact, Jura (1994) has argued that in order to explain the observed circumstellar polarization of the archetypical carbon star IRC+10216 such a modified distribution is required, with $a_0 \approx 0.10$ μm, which allows for a sufficiently large number of grains >1 μm in diameter. However, the grain size distribution observed by Amari et al. (1994) is not consistent with this modified MRN law for any reasonable choice of a_0 either. Remarkably, though, it is consistent with predictions (Dominik et al. 1989) for the size distribution of dust particles formed in a dust-driven wind from a carbon star, which has the form of a power law with an exponent b in the range 5 to 7 (versus 5.7 for Murchison SiC). The predicted distribution is expected to describe the distribution of grains in the size range from 0.005 μm up to about 10 μm, as they are injected into the interstellar medium (Dominik et al. 1989).

Stellar Consequences

Alexander (1993), based on a (compared to today) incomplete database on meteoritic SiC grains concluded that at least some ten, but maybe hundreds of different AGB stars contributed to the inventory of presolar SiC grains found in primitive meteorites. This fact, most strongly required by the variation in Si isotopes (e.g., Timmes and Clayton 1996; Hoppe and Ott 1997; Lugaro et al. 1999), has been confirmed by all subsequent studies. A corollary of a short exposure age (as well as of their unprocessed nature) is that grains from all the various stellar sources must have been collected in a relatively short time. Although not dealing with this aspect, the work of Clayton (2003) concerning the problem of silicon isotopes may offer a possible solution.

In Clayton's scenario, the merger of a metal-poor satellite galaxy with the Milky Way about 5.5–6.5 Ga ago caused a starburst. Stars that formed almost simultaneously at this time became AGB stars about 1–2 Ga later and donated SiC grains to the interstellar medium at the solar radius of the galaxy. Important in our context is the time scale of stellar evolution. Isotopic compositions of trace elements made in the s-process indicate that those stars were of low mass between 1.5 and 2.5 $M_\odot$ (e.g., Savina et al. 2003). Stellar lifetimes classically scale with $M^{-2.5}$, with a somewhat larger exponent of 2.7 suggested by a recent re-determination of the mass-luminosity relationship based on Hipparcos data by Martin et al. (1998). Hence, only a fraction of those stars (with M larger than about 2 $M_\odot$, living less than 1.5 Ga) may have made it to the AGB stage within the timeframe suggested by Clayton's model. Almost none of them can have produced SiC grains that were of old age at the time of solar system formation. In fact, what we see in the meteorites may only be the first arrivals of SiC grains—just recently formed before the Sun's birth—from all those stars whose formation was triggered by that suggested galactic merger.

Although suggestive of a short cosmic ray exposure for SiC of all grain sizes, constraints are most severe for the largest ones, KJE of average grain size 1.14 μm and KJF of average grain size 1.86 μm (Figs. 8a and 8b). Sensitivity is

lower for the finer grains because of their higher abundance of trapped Xe gas. Also the SEM study of Bernatowicz et al. (2003), strictly speaking, proves the rather unprocessed nature of grains larger than 0.8 μm only. It is possible, therefore, that the smaller grains were exposed in the interstellar medium for longer times or that, in fact, they constitute the remains of once larger, older grains. If so, and if the above (admittedly speculative) connection to a galactic merger causing a burst of star formation is correct, the well-established dependence of various mean isotopic compositions on grain size (Hoppe et al. 1996; Lewis et al 1990, 1994; Amari et al. 1996; Podosek et al. 2004; Prombo et al. 1993) may be related to the time when those stars became AGB stars and hence, ultimately, may be related to their mass. It may be interesting to check in detail, if the variations follow the trends expected from varying stellar masses. This is not a trivial task, since expectations sensitively depend not only on mass but also on the metallicity of the parent stars. It will undoubtedly be difficult to disentangle the influence of the two, but this is beyond the scope of this paper, anyway.

SUMMARY

To gain insight into the presolar life of the SiC grains found in primitive meteorites, we have determined the recoil range for spallation xenon produced by proton irradiation of Ba glass targets. This was done by the catcher technique, where spallation Xe was measured in the Ba glass targets and in catcher foils collecting the recoil nuclei emitted from the target. Important results are:

- The recoil of ^{126}Xe range in our Ba glass (~40 wt% Ba) was determined in two experiments, at different energies, 268 MeV and 1190 MeV (at the target). Small differences may exist between the ranges observed in the two irradiations. The average range in Ba glass of ~0.23 μm corresponds to a range in SiC of ~0.19 μm according to range-energy relations (Ziegler 2003).
- Based on this range, we infer retention of spallation ^{126}Xe in a typical grain of size 1 μm to be ~70%. This includes allowance for range straggling as well as the effects of variations in recoil energy and deviations from spherical shape of the grains, by artificially including 40% "effective straggling".
- Recoil ranges are different for the different Xe isotopes, correlating with the mass difference between target and product nuclei.
- Data obtained from an irradiation at low energy (~66 MeV at the target) are not very precise, but there is no indication for a significantly different recoil range at this energy.

We have used the experimental data to put constraints on the possible presolar age of the SiC grains analyzed for Xe by Lewis et al. (1994). Our conclusions are:

- Uncertainties in retention are no longer an issue; more serious problems for determining a presolar cosmic ray exposure age are uncertainties in the production rate in the interstellar medium, and, even more importantly, in the composition of the approximately normal Xe component in SiC (Xe-N).
- For the largest grain sizes, cosmogenic ^{126}Xe produced during the expected lifetime of interstellar SiC exceed the total amount of ^{126}Xe present. Based on "reasonable" assumptions for the production rates and the ^{124}Xe/^{126}Xe ratio in Xe-N (e.g., Xe-Q-like), we calculate nominal exposure ages also for the other size fractions that are considerably shorter than theoretically expected lifetimes for interstellar grains.
- A possible interpretation, and maybe the most likely, is that spallation contributions are negligible and that ^{124}Xe/^{126}Xe in Xe-N is ~5% lower than in Q-Xe.
- A short presolar age is in line with observations by other workers that indicate very little processing in the interstellar medium of surviving SiC.
- Amorphization of presolar grains may occur in the ISM on a much shorter time scale than destruction (cf. Kemper et al. 2004); because amorphous SiC may not have survived in the early solar system, the time scale for amorphization may be more relevant than the destruction time scale for comparison with the cosmic ray exposure age.
- A large supply of relatively young grains may be in line with the suggestion (Clayton 2003) of a starburst origin for the parent stars of the SiC mainstream grains ~1-2 Ga before solar system formation.

Acknowledgments–We are grateful to the Laboratory National Saturne/Saclay and the Paul Scherrer Institute/Villigen for making available the irradiations and to the staffs of the laboratories for kind cooperation and support. The noble gas mass spectrometer was maintained by S. Herrmann, who also assisted in the operation. E. Anders (unintentionally and probably unknowingly) and F. Begemann stimulated our interest in the problem of recoil losses of spallation products. Constructive reviews by R. Wieler and an anonymous reviewer are acknowledged.

Editorial Handling—Dr. Marc Caffee

REFERENCES

Alexander C. M. O'D. 1993. Presolar SiC in chondrites: How variable and how many sources? *Geochimica et Cosmochimica Acta* 57:2869–2888.

Amari S., Lewis R. S., and Anders E. 1994. Interstellar grains in meteorites: I. Isolation of SiC, graphite, and diamond; size distributions of SiC and graphite. *Geochimica et Cosmochimica Acta* 58:459–470.

Amari S., Zinner E., and Lewis R. S. 1996. Ca and Ti isotopic

compositions of size-separated SiC fractions from the Murchison meteorite (abstract). 27th Lunar and Planetary Science Conference. pp. 23–24.

Bernatowicz T. J. and Zinner E., editors. 1997. *Astrophysical implications of the laboratory study of presolar materials*. Woodbury, New York: American Institute of Physics. 750 p.

Bernatowicz T., Messenger S., Pravdivtseva O., Swan P., and Walker R. M. 2003. Pristine presolar silicon carbide. *Geochimica et Cosmochimica Acta* 67:4679–4691.

Bodemann R., Lange H.-J., Leya I., Michel R., Schiekel T., Rösel R., Herpers U., Hofmann H. J., Dittrich B., Suter M., Wölfli W., Holmqvist B., Condé H., and Malmborg P. 1993. Production of residual nuclei by proton-induced reactions on C, N, O, Mg, Al and Si. *Nuclear Instruments and Methods in Physics Research B* 82:9–31.

Boss A. P. and Foster P. N. 1997. Triggering presolar cloud collapse and injecting material into the presolar nebula. In *Astrophysical implications of the laboratory study of presolar materials*, edited by Bernatowicz T. J. and Zinner E. Woodbury, New York: American Institute of Physics. pp. 649–664.

Busemann H., Baur H., and Wieler R. 2000. Primordial noble gases in "phase Q" in carbonaceous and ordinary chondrites studied by closed-system stepped etching. *Meteoritics & Planetary Science* 35:949–973.

Castagnoli G. and Lal D. 1980. Solar modulation effects in terrestrial production of carbon-14. *Radiocarbon* 22:133–159.

Clayton D. D. 2003. A presolar galactic merger spawned the SiC-grain mainstream. *The Astrophysical Journal* 598:313–324.

Dominik C., Gail H.-P., and Sedlmayr E. 1989. The size distribution of dust particles in a dust-driven wind. *Astronomy & Astrophysics* 223:227–236.

Draine B. T. 2003. Interstellar dust grains. *Annual Review of Astronomy and Astrophysic*s 41:241–289.

Eugster O. 1988. Cosmic-ray production rates for ^{3}He, ^{21}Ne, ^{38}Ar, ^{83}Kr, and ^{126}Xe in chondrites based on ^{81}Kr-Kr exposure ages. *Geochimica et Cosmochimica Acta* 52:1649–1662.

Foster P. N. and Boss A. P. 1996. Triggering star formation with stellar ejecta. *The Astrophysical Journal* 468:784–796.

Funk H. and Rowe M. W. 1967. Spallation yield of xenon from 730 MeV proton irradiation of barium. *Earth and Planetary Science Letters* 2:215–219.

Gallino R., Busso M., Picchio G., and Raiteri C. M. 1990. On the astrophysical interpretation of isotope anomalies in meteoritic SiC grains. *Nature* 348:298–302.

Gilabert E., Lavielle B., Schiekel Th., Herpers U., Neumann S., Leya I., and Michel R. 1997. Measurements and modeling the production of krypton and xenon in a simulation experiment of an artificial iron meteoroid: application to the chondrite Knyahinya (abstract). *Meteoritics & Planetary Science* 32:A47–A48.

Gloris M., Michel R., Sudbrock F., Herpers U., Malmborg P., and Holmqvist B. 2001. Proton-induced production of residual radionuclides in lead at intermediate energies. *Nuclear Instuments and Methods in Physics Research A* 463:593–633.

Hohenberg C. M., Hudson B., Kennedy B. M., and Podosek F. A. 1981. Xenon spallation systematics in Angra dos Reis. *Geochimica et Cosmochimica Acta* 45:1909–1915.

Hoppe P. and Ott U. 1997. Mainstream silicon carbide grains from meteorites In *Astrophysical implications of the laboratory study of presolar materials*, edited by Bernatowicz T. J. and Zinner E. Woodbury, New York: American Institute of Physics. pp. 27–58.

Hoppe P. and Zinner E. 2000. Presolar dust grains from meteorites and their stellar sources. *Journal of Geophysical Research A* 105: 10,371–10,385.

Hoppe P., Strebel R., Eberhardt P., Amari S., and Lewis R. S. 1996. Small SiC grains and a nitride grain of circumstellar origin from the Murchison meteorite: Implications for stellar evolution and nucleosynthesis. *Geochimica et Cosmochimica Acta* 60:883–907.

Huss G. R. and Lewis R. S. 1994. Noble gases in presolar diamonds I: Three distinct components and their implications for diamond origins. *Meteoritics* 29:791–810.

Huss G. R., Lewis R. S., and Hemkin S. 1996. The "normal planetary" noble gas component in primitive chondrites: Compositions, carrier and metamorphic history. *Geochimica et Cosmochimica Acta* 60:3311–3340.

Ip W.-H. and Axford W. I. 1985. Estimates of galactic cosmic ray spectra at low energies. *Astronomy & Astrophysics* 149:7–10.

Jones A. P., Tielens A. G. G. M., Hollenbach D. J., and McKee C. F. 1994. Grain destruction in shocks in the interstellar medium. *The Astrophysical Journal* 433:797–810.

Jones A. P., Tielens A. G. G. M., Hollenbach, D. J., and McKee C. F. 1997. The propagation and survival of interstellar grains. In *Astrophysical implications of the laboratory study of presolar materials*, edited by Bernatowicz T. J. and Zinner E. Woodbury, New York: American Institute of Physics. pp. 595–613.

Jura M. 1994. The particle-size distribution in the dust ejected from IRC+10216. *The Astrophysical Journal* 434:713–718.

Kaiser W. A. 1977. The excitation functions of Ba(p,X)^{M}Xe (M = 124–136) in the energy range 38–600 MeV: The use of 'cosmogenic' xenon for estimating 'burial' depths and 'real' exposure ages. *Philosophical Transactions of the Royal Society of London A* 285:337–362.

Kemper F., Vriend W. J., and Tielens A. G. G. M. 2004. The absence of crystalline silicates in the diffuse interstellar medium. *The Astrophysical Journal* 609:826–837.

Lagarde-Simonoff M., Regnier S., Sauvageon H., and Simonoff G. N. 1976. Recoil properties of spallation products from bombardment of Z = 13–29 targets with 150, 300 and 600 MeV protons. *Nuclear Physics A* 260:369–380.

Lange H.-J., Hahn T., Michel R., Schiekel T., Rösel R., Herpers U., Hofmann H.-J., Dittrich-Hannen B., Suter M., Wölfli W., and Kubik P. W. 1995. Production of residual nuclei by α-induced reactions on C, N, O, Mg, Al and Si up to 170 MeV. *Applied Radiation and Isotopes* 46:93–112.

Lewis R. S., Amari S., and Anders E. 1990. Meteoritic silicon carbide: Pristine material from carbon stars. *Nature* 348:293–298.

Lewis R. S., Amari S., and Anders E. 1994. Interstellar grains in meteorites: II. SiC and its noble gases. *Geochimica et Cosmochimica Acta* 58:471–494.

Leya I., Lange H.-J., Neumann S., Wieler R., and Michel R. 2000. The production of cosmogenic nuclides in stony meteoroids by galactic cosmic-ray particles. *Meteoritics & Planetary Science* 35:259–286.

Lugaro M., Zinner E., Gallino R., and Amari S. 1999. Si isotopic ratios in mainstream presolar SiC grains revisited. *The Astrophysical Journal* 527:369–394.

Martin C., Mignard F., Hartkopf W. I., and McAlister H. A. 1998. Mass determination of astrometric binaries with Hipparcos. *Astronomy & Astrophysics* 133:149–162.

Mathew K. J., Rao M. N., Weber H. W., Herpers U., and Michel R. 1994. Xenon production cross sections at intermediate energies and production rates in small meteoroids based on simulation experiments. *Nuclear Instruments and Methods in Physics Research B* 94:449–474.

Mathis J. S., Rumpl W., and Nordsieck K. H. 1977. The size distribution of interstellar grains. *The Astrophysical Journal* 217: 425–433.

Mendybaev R. A., Beckett J. R., Grossman L., Stolper E., Cooper R. F., and Bradley J. P. 2002. Volatilization kinetics of silicon

carbide in reducing gases: An experimental study with applications to the survival of presolar grains in the solar nebula. *Geochimica et Cosmochimica Acta* 66:661–682.

Messenger S., Keller L. P, Stadermann F. J., Walker R. M., and Zinner E. 2003. Samples of stars beyond the solar system: Silicate grains in interplanetary dust. *Science* 300:105–108.

Michel R., Dragovitsch P., Cloth P., Dagge G., and Filges D. 1991. On the production of cosmogenic nuclides in meteoroids by galactic protons. *Meteoritics* 26:221–242.

Michel R., Gloris M., Lange H.-J., Leya I., Lüpke M., Herpers U., Dittrich-Hannen B., Rösel R., Schiekel Th., Filges D., Dragovitsch P., Suter M., Hofmann H.-J., Wölfli W., Kubik P. W., Baur H., and Wieler R. 1995. Nuclide production by proton-induced reactions on elements ($6 \le Z \le 29$) in the energy range from 800 MeV to 2600 MeV. *Nuclear Instruments and Methods in Physics Research B* 103:183–222.

Michel R., Bodemann R., Busemann H., Daunke R., Gloris M., Lange H.-J., Klug B., Krins A., Leya I., Lüpke M., Neumann S., Reinhard, H., Schnatz-Büttgen M., Herpers U., Schiekel Th., Sudbrock F., Holmqvist B., Condé H., Malmborg P., Suter M., Dittrich-Hannen B., Kubik P.-W., Synal H.-A., and Filges D. 1997. Cross sections for the production of residual nuclides by low- and medium-energy protons from the target elements C, N, O, Mg, Al, Si, Ca, Ti, V, Mn, Fe, Co, Ni, Cu, Sr, Y, Zr, Nb, Ba and Au. *Nuclear Instruments and Methods in Physics Research B* 129:153–193.

Mohapatra R., Merchel S., Ott U., Herpers U., and Michel R. 2001. Recoil of spallation xenon: Hope for dating presolar SiC (abstract #1296). 32nd Lunar and Planetary Science Conference. CD-ROM.

Mostefaoui S. and Hoppe P. 2004. Discovery of abundant in situ silicate and spinel grains from red giant stars in a primitive meteorite. *The Astrophysical Journal* 613:L149–L152.

Nagashima K., Krot A. N., and Yurimoto H. 2004. Stardust silicates from primitive meteorites. *Nature* 428:921–924.

Nguyen A. and Zinner E. 2004. Discovery of ancient silicate stardust in a meteorite. *Science* 303:1496–1499.

Ott U. 2002 Noble gases in meteorites–Trapped components. In *Noble gases in geochemistry and cosmochemistry*, edited by Porcelli D., Ballentine C. J., and Wieler R. Washington, D.C.: Mineralogical Society of America. pp. 71–100.

Ott U. 2003. The most primitive material in meteorites. In *Astromineralogy*, edited by Henning Th. Berlin: Springer. pp. 236–265.

Ott U. and Begemann F. 2000. Spallation recoil and age of presolar grains in meteorites. *Meteoritics & Planetary Science* 35:53–63.

Ott U., Altmaier M., Herpers U., Kuhnhenn J., Merchel S., Michel R., and Mohatara R. K. 2001. Update on recoil loss of spallation products from presolar grains (abstract). *Meteoritics & Planetary Science* 36:A155–A156.

Pepin R. O., Becker R. H., and Rider P. E. 1995. Xenon and krypton isotopes in extraterrestrial regolith soils and in the solar wind. *Geochimica et Cosmochimica Acta* 59:4997–5022.

Podosek F. A., Prombo C. A., Amari S., and Lewis R. S. 2004. S-process Sr isotopic compositions in presolar SiC from the Murchison meteorite. *The Astrophysical Journal* 605:960–965.

Prescher K., Peiffer F., Stueck R., Michel R., Bodemann R., Rao M. N., and Mathew K. J. 1991. Thin-target cross sections of proton-induced reactions on barium and solar cosmic ray production rates of xenon-isotopes in lunar surface materials. *Nuclear Instruments and Methods in Physics Research B* 53: 105–121.

Prombo C. A., Podosek F. A., Amari S., and Lewis R. S. 1993. S-process Ba isotopic compositions in presolar SiC from the Murchison meteorite. *The Astrophysical Journal* 410:393–399.

Reedy R. C. 1987. Nuclide production by primary cosmic-ray protons. Proceedings, 17th Lunar and Planetary Science Conference. *Journal of Geophysical Research* 92:E697–E702.

Reedy R. C. 1989. Cosmogenic-nuclide production rates in interstellar grains (abstract). 30th Lunar and Planetary Science Conference. pp. 888–889.

Schelhaas N., Ott U., and Begemann F. 1990. Trapped noble gases in unequilibrated ordinary chondrites. *Geochimica et Cosmochimica Acta* 54:2869–2882.

Schiekel Th., Sudbrock F., Herpers U., Gloris M., Lange H.-J., Leya I., Michel R., Dittrich-Hannen B., Synal H.-A., Suter M., Kubik P. W., Blann M., and Filges D. 1996. Nuclide production by proton-induced reactions on elements ($6 \le Z \le 29$) in the energy range from 200 MeV to 400 MeV. *Nuclear Instruments and Methods in Physics Research B* 114:91–119.

Shukolyukov A. Yu. and Gorin V. D. 1988. Xenon isotope yields from Cs, Ba, and REE produced by protons at 72 and 100 MeV and 1 GeV. *Geochemistry International* 25:110–114.

Simpson J. A. 1983. Elemental and isotopic composition of the galactic cosmic rays. *Annual Review of Nuclear and Particle Science* 33:323–381.

Steinberg E. P. and Winsberg L. 1974. Recoil properties of ^{22}Na and ^{24}Na produced in the interaction of ^{27}Al with 3- to 300-GeV protons. *Physical Review C* 10:1925–1927.

Straniero O., Chieffi A., Limongi M., Busso M., Gallino R., and Arlandini C. 1997. Evolution and nucleosynthesis in low-mass asymptotic giant branch stars. I. Formation of population I carbon stars. *The Astrophysical Journal* 478:332–339.

Sugarman N., Campos M., and Wielgoz K. 1956. Recoil studies of high-energy proton reactions in bismuth. *Physical Review* 101: 388–397.

Tang M. and Anders E. 1988a. Isotopic anomalies of Ne, Xe, and C in meteorites. III. Local and exotic noble gas components and their interrelations. *Geochimica et Cosmochimica Acta* 52:1245–1254.

Tang M. and Anders E. 1988b. Interstellar silicon carbide: How much older than the solar system? *The Astrophysical Journal* 335:L31–L34.

Timmes F. X. and Clayton D. D. 1996. Galactic evolution of silicon isotopes: application to presolar SiC grains from meteorites. *The Astrophysical Journal* 472:723–741.

Walton J. R., Heymann D., Yaniv A., Edgerley D., and Rowe M. W. 1976. Cross sections for He and Ne isotopes in natural Mg, Al and Si, He isotopes in CaF_2, and radionuclides in natural Al, Si, Ti, Cr, and stainless steel induced by 12–45 MeV protons. *Journal of Geophysical Research* 81:5689–5699.

Webber W. R. and Yushak S. M. 1983. A measurement of the energy spectra and relative abundance of the cosmic-ray H and He isotopes over a broad energy range. *The Astrophysical Journal* 275:391–404.

Whittet D. C. B. 2003. *Dust in the galactic environment*. Bristol and Philadelphia: IOP Publishing. 390 p.

Wieler R. 2002. Noble gases in the solar system. In *Noble gases in geochemistry and cosmochemistry*, edited by Porcelli D., Ballentine C. J., and Wieler R. Washington D.C.: Mineralogical Society of America. pp. 21–70.

Ziegler J. F. 2003 SRIM-2003. *Nuclear Instruments and Methods in Physics Research B* 219:1027–1036.

Zinner E., Amari S., and Lewis R. S. 1991. S-process Ba, Nd, and Sm in presolar SiC from the Murchison meteorite. *The Astrophysical Journal* 382:L47–L50.